Journal of Macromolecular Science, Part A
Publication details, including instructions for authors and subscription information:
http://www.informaworld.com/smpp/title~content=t713597274

Designing EPDM Products for Extrusion Applications

N. P. Cheremisinoff[a]
[a] Exxon Chemical Company Linden, New Jersey

To cite this Article Cheremisinoff, N. P.(1989) 'Designing EPDM Products for Extrusion Applications', Journal of Macromolecular Science, Part A, 26: 8, 1231 — 1259
To link to this Article: DOI: 10.1080/00222338908052044
URL: http://dx.doi.org/10.1080/00222338908052044

J. MACROMOL. SCI.—CHEM., A26(8), pp. 1231-1259 (1989)

DESIGNING EPDM PRODUCTS FOR EXTRUSION APPLICATIONS

N. P. CHEREMISINOFF

Exxon Chemical Company
Linden, New Jersey 07036

ABSTRACT

An experimental investigation was aimed at understanding extrusion operating parameters and polymer properties important to the skin surface appearance of extruded EPDM products. The purpose of this study was to develop general guidelines that can be applied to the design of new products in sponge and/or dense profiles for a variety of consumer applications, including automotive weatherstrips. In many of these applications, cure and physical properties as well as extrusion performance in terms of high line rates, low swell, and smooth surface appearance are important. This paper concerns the relationships between the hydrodynamics of extrusion and skin appearance as well as the desirable molecular characteristics for achieving smooth skin surface. The study shows that polymers with broader molecular weight distributions have a significant advantage in processing latitude over those of narrow molecular weight distribution, with skin appearance shown to depend on the extent of viscous heating during the forming operation.

INTRODUCTION AND BACKGROUND

The aesthetic qualities of extruded articles are critical in many consumer-oriented applications. One area where this has become a major concern is in the manufacture of various automotive rubber parts, such as glass run channels, weatherstrip seals, trunk seals, and others. Such parts are being required to

stand up to increasingly more stringent warranties in providing multifunctional sealing, maintaining tight dimensional control with rather complex part profiles, and being able to be produced at relatively high extrusion line speeds. The vast majority of these parts are manufactured from EPDM polymers (ethylene-propylene-diene rubber). These terpolymers have been extensively used in manufacturing a variety of extrusion articles for over a quarter of a century because of their wide processing latitude and excellent resistance to ozone, weathering, and heat, in combination with their good physical properties.

Ethylene and propylene are the basic monomers of this polymer, with polymerization performed in the presence of a transition-metal halide/aluminum alkyl catalyst. The product is a high molecular weight elastomer. The use of a third monomer or diene (in this study ethylidenenorbornene (ENB)) provides unsaturated functionality along the polymer chain to increase vulcanization response with peroxide curing systems or to make the rubber sulfur curable. The diene polymerizes through a strained ring resulting in a carbon-carbon double bond pendent to the main chain. The excellent weathering and ozone resistance of these polymers is attributed to the completely saturated backbone.

In extrusion applications such as described here, the rubber must have ultrafast curing rates in order to achieve economic cure cycles and parts with low compression set for good sealing. Furthermore, they must be relatively high in molecular weight in order to provide good shape retention and maintain dimensional stability as rather complex parts profiles [3, 6]. Slow-curing polymers have the advantage that they are less sensitive to process shear rates and high temperatures, resulting in smooth, aesthetically pleasing cured vulcanizate surfaces, but at the cost of uneconomical line rates. Understanding the polymer and process technology required to produce a continuously cured part which meets the end user's requirements, namely low compression set, excellent shape retention, and a smooth finished part surface, is critical to the design and/or selection of the proper rubber. This requires an understanding of the extrusion process, which in turn helps to define the desired rheological response of the compound polymer. With the proper rheology and viscoelastic properties defined, polymers can be more rationally designed in terms of their molecular weight, molecular weight distribution, and composition.

This paper focuses on the extrusion parameters and important molecular properties that establish good skin appearance for dense profiles. In addition to the polymer properties and the extrusion conditions, such factors as the degree of ingredient dispersion in the rubber, the continuous vulcanization medium, the profile complexity, and the postforming operations also influence these performance parameters.

EXPERIMENTAL SET-UP AND CONDITIONS

The present study was performed on a number of EPDM elastomers, all compounded in a conventional weatherstrip formulation. The properties of the test samples are reported in Table 1. Masterbatches were extruded in a Haake System 40 torque rheometer at several temperatures over a range of screw speeds. The extruder section of the rheocord is a single-screw mixer with a screw diameter of 25 mm and a length-to-diameter ratio of 20. The unit is equipped with dual thermocouple/piezoelectric wall tap transducers, located at three axial locations for simultaneous measurements of melt temperature and static wall pressure. In addition, the unit measures the instantaneous torque response of the rotor shaft, which is a measure of the force required for extrusion per revolution.

Compound stocks were extruded through a standard Garvey die. Extrudate swell as well as mass and linear rates were measured. A qualitative rating of the surface appearance/texture was recorded for each set of operating conditions. The qualitative rating is based on an elaboration of the conventional Garvey die extrudate rating system for surface, in that finer distinctions were made instead of the customary four-point system (1 = poor, 2 = fair, 3 = good, 4 = smooth). Figure 1 illustrates the classification system and the definitions adopted in this study.

DEVELOPMENT OF CONSTITUTIVE EQUATIONS FOR THE TORQUE RHEOMETER

The torque rheometer is a processability tester which characterizes the processing rheology of elastomeric and plastic materials. Since the torque exerted by the rotor shaft in turning the screw of the extruder section is measured, the instrument provides an indirect measure of the stresses or the average apparent viscosity of the polymer over the entire extruder section. This viscosity measurement is, however, not the same as that made for simple shear flow in a device such as a capillary rheometer, because of obvious geometric differences in flow geometry and because polymer rheological properties vary from inlet to discharge. In this regard, the principal difference is that a capillary rheometer provides a measure of the steady-state melt stress as determined under isothermal conditions (as derived from a momentum balance), whereas the torque rheometer indirectly measures an average stress under adiabatic conditions. Further, since the geometry of the rheocord is complex compared to a capillary, rigorous expressions relating torque to melt-state stress are not pos-

TABLE 1. Properties of Polymers Studied

Polymer identification	Symbol on plots	Mooney viscosity (1′ + 4′) 125°C	Oil, phr	Propylene content, wt%	ENB content relative to Polymer A
A	○ ϕ	50	50	50	High
B	□	67	–	57	0.98
C	●	71	–	69.9	1.07
D	△	66	–	66	0.99
E	▽	72	75	70	1.00
F	▲	93	–	62	1.04
G	▼	92	–	62	1.00
J	▷	36	30	58	0.97
K	○	88	–	60.5	0.94
L	○	103	–	63	0.79
M	○	98	–	62	0.90
N	■	98	–	62.6	0.89
O	◇	88	–	58.2	0.88
P	●	78	–	61.1	0.91

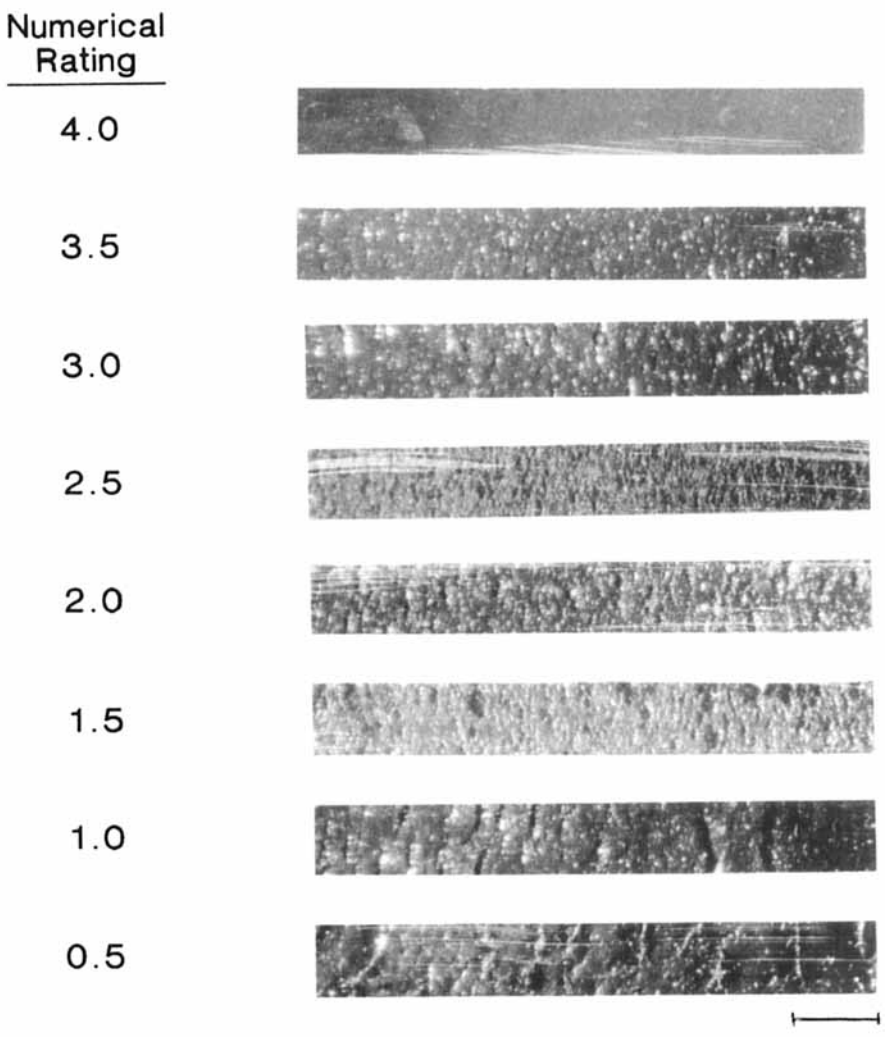

FIG. 1. Surface appearance rating chart used for study. The size bar represents 1 mm and the photographs are at 14X magnification.

sible. It is, however, possible to derive some practical expressions that can be applied to processing performance scale-up. The first fundamental parameter derived for the rheocord is the torque, which in simple terms is the effectiveness of a force to produce rotation. It is the product of force and the perpendicular distance from its line of action to the instantaneous center of rotation, i.e.,

$$\tau = F \times r, \tag{1}$$

where τ is the torque in g·m, dyn·cm, or lb·ft, r is the radius, and F is the force.

The power (P) is the time rate at which work is done:

$$P = F \times V, \tag{2}$$

where V is the rotational velocity.

From the above, the torque for the rheocord can be related to shaft horsepower, hp, and the rotation rate, rpm (min^{-1}), by

$$\tau = 725\ 995 \times \text{hp/rpm}, \tag{3}$$

where τ has units of m·g.

Total shear energy, TE, is the energy introduced to the polymer by the motor drive during processing. It is computed from the measured torque times the screw speed N.

$$TE = \tau \times N \times 9.803 \times 10^{-3}. \tag{4}$$

This definition provides information on the total mechanical energy required to process the material.

Specific energy, SE, is the energy required to process a unit mass of material. It is the total shear energy divided by the total mass flow rate m:

$$SE = 0.0167TE/m. \tag{5}$$

The specific energy provides information on the viscous dissipation heat build-up in the system based on screw speed.

Specific output, SO, is defined as the mass flow rate per unit rpm of the screw:

$$SO = m/N. \tag{6}$$

This parameter provides information on the uniformity of solids conveying, melting, and pumping mechanisms, characteristic of the particular screw geometry used.

Shear rate will vary over the extruder screw. By convention, shear rate is referred to as the shear rate in the metering section of the screw, defined by

$$\dot{\gamma} = \pi DN/h, \tag{7}$$

where D is the screw diameter, N is the rpm, and h is the gap between the screw and the barrel.

Three different screw geometries were used (see Fig. 2).

A final definition, based on analogy to simple shear flow, for the processing viscosity is presented. Torque contains information on shear stress, and therefore can be correlated with the shear rate definition of Eq. (7) through a power-law relation:

$$\tau = K\dot{\gamma}^n, \tag{8}$$

where K depends on screw geometry as well as on polymer melt characteristics. On combining Eq. (8) with Newton's law, an expression for processing (apparent) viscosity can be obtained:

$$\eta_p = K\dot{\gamma}^{n-1}. \tag{9}$$

We assume here that shear stresses, τ, in the melt and the torque measured by the rheocord are equivalent, which, of course, is not strictly true. Nonetheless, we are able to obtain a value of processing viscosity which is specific to the rheocord geometry as computed from the regression coefficients of Eq. (8). See Chung [4] and Cheremisinoff [1] for further discussions on torque rheometry. The following expression can be further derived by combining the power law expression with the Arrhenius relation, to account for temperature effects.

$$\tau = k\left[\dot{\gamma}\exp\left(\frac{\Delta E}{RT}\right)\right]^n. \tag{10A}$$

Expressing this relation as a two-variable polynomial, we obtain

$$\ln(\tau) = \ln(k) + n\ln(\dot{\gamma}) + \left(\frac{n\Delta E}{R}\right)\left(\frac{1}{T}\right), \tag{10B}$$

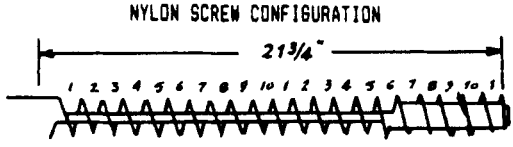

POS.	DIA.(in)	POS.	DIA.(in)	POS.	DIA.(in)
1	0.625	1	0.630	1	0.900
2	0.625	2	0.630		
3	0.625	3	0.630		
4	0.625	4	0.630		
5	0.628	5	0.630		
6	0.628	6	0.630		
7	0.628	7	0.875		
8	0.630	8	0.900		
9	0.630	9	0.900		
10	0.630	10	0.900		

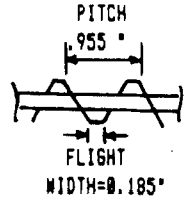

(a)

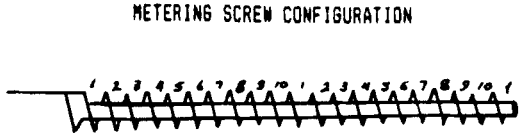

POS.	DIA.(in)	POS.	DIA.(in)	POS.	DIA.(in)
1	0.618	1	0.630	1	0.874
2	0.622	2	0.665		
3	0.624	3	0.713		
4	0.626	4	0.746	PITCH= 1"	
5	0.626	5	0.791		
6	0.626	6	0.795	FLIGHT WIDTH= 0.181"	
7	0.632	7	0.870		
8	0.632	8	0.872		
9	0.632	9	0.872		
10	0.630	10	0.872		

(b)

FIG. 2. Screw configurations used in study.

3:1 COMPRESSION SCREW

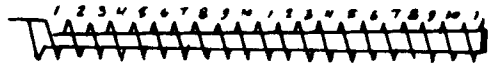

POS.	DIA. (in)	POS.	DIA. (in)	POS.	DIA. (in)
1	0.615	1	0.752	1	0.870
2	0.630	2	0.767		
3	0.650	3	0.780		
4	0.668	4	0.792	PITCH= 1"	
5	0.672	5	0.805		
6	0.690	6	0.820	FLIGHT WIDTH= 0.175"	
7	0.705	7	0.825		
8	0.720	8	0.840		
9	0.730	9	0.855		
10	0.740	10	0.864		

(c)

FIG. 2 (continued)

where $\dot{\gamma}$ and $1/T$ are independent variables, and k and (nE/R) are property constants. As shown, these parameters can be related to molecular properties of the polymers and, therefore, provide a link to processability scale-up.

Figure 3 illustrates the wide range of processability observed between polymer candidates by a plot of measured torque versus shear rate. By applying linear regression (Eq. 10B), the property coefficients can be readily evaluated. It is observed that the unity shear viscosity coefficient, k, is a strong function of the weight-average molecular weight as measured by gel-permeation chromatography (GPC) (refer to Fig. 4). As one would expect, the viscosity increases with molecular weight. The activation energy of flow $(\Delta E/R)$ is also shown to be a function of molecular weight (refer to Fig. 5). In this case a decreasing function is observed which is consistent with processing observations; specifically, higher molecular weight polymers generally require more work to induce deformation and, hence, one would expect a lower ΔE. The power-law index, n, was shown in prior studies [2] to be a function of molecular weight, molecular weight distribution (particularly sensitive to the high ends of the molecular weight distribution), and the extent of long-chain branching.

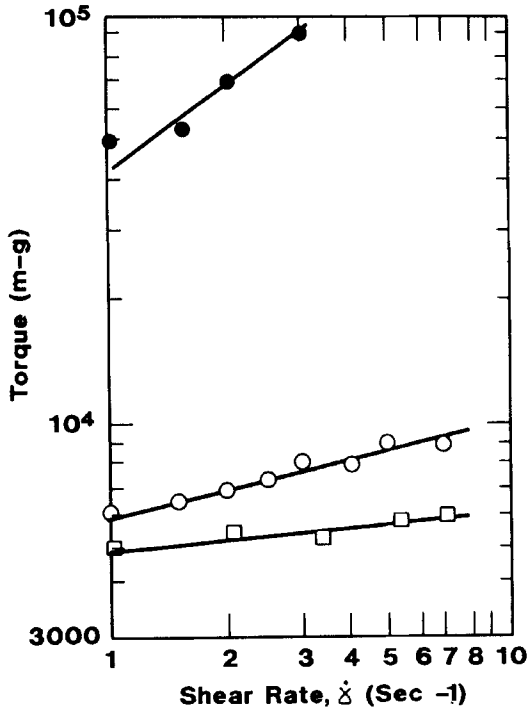

FIG. 3. Plot of torque versus shear rate for three polymers (constant wall temperature of 90°C).

Parameters n, E, and k are independent of temperature. We can conclude that Eq. (10B) provides a proper physical model of the extrusion process in terms of shear stress (torque) or a calculated processing melt viscosity. Furthermore, the sensitivity of the model to molecular properties provides guidance in designing the polymer for certain processing advantages, such as fast extrusion.

RELATION BETWEEN EXTRUSION AND SKIN APPEARANCE

Skin appearance materializes as a melt-fracture phenomenon which can be related to viscous heating effects. Figure 6 shows a plot of surface rating versus the temperature rise due to viscous heating (i.e., the difference between melt temperature and extruder barrel wall temperature) in one polymer candidate.

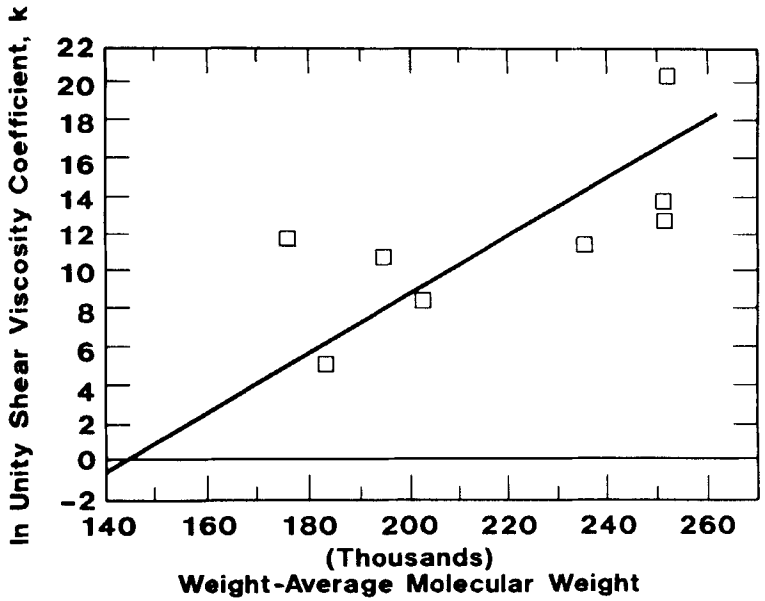

FIG. 4. Semilogarithmic plot of k vs weight-average molecular weight (from GPC).

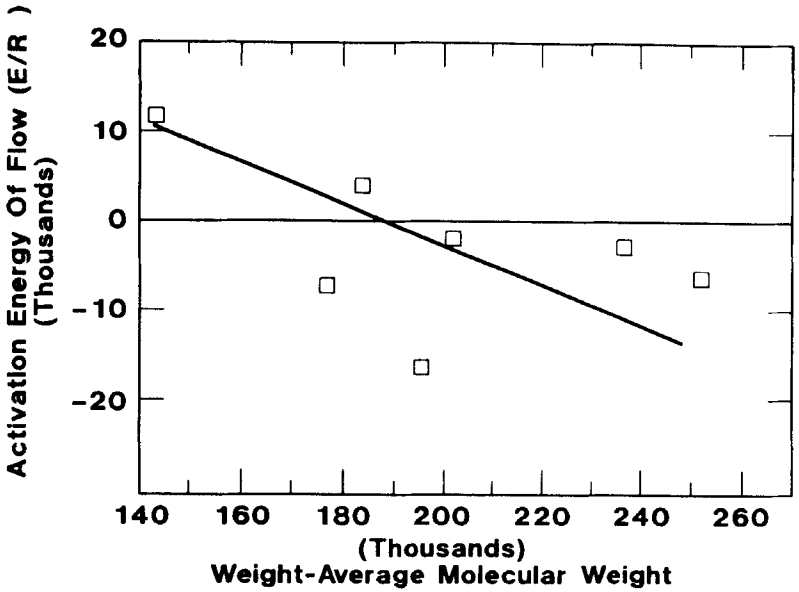

FIG. 5. Activation energy of flow vs molecular weight (from GPC).

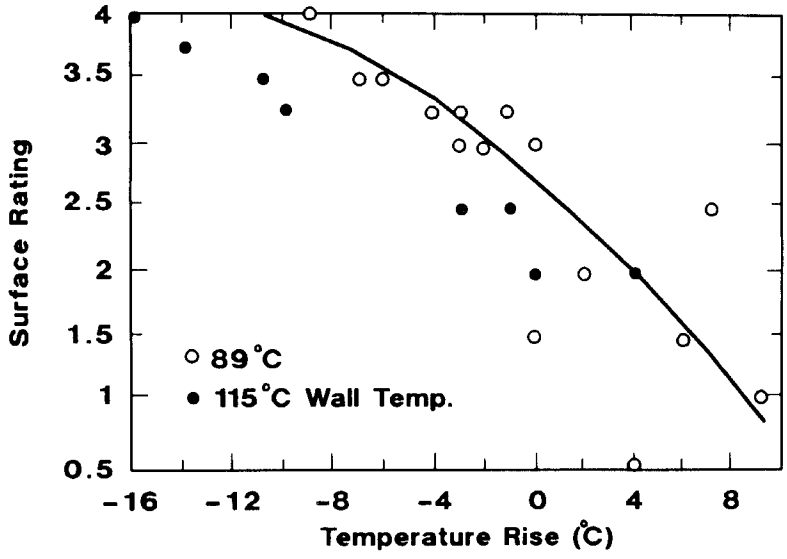

FIG. 6. Viscous heating effect on skin appearance for Polymer A.

These data were generated over different screw rpm's. Figure 6 simply illustrates that as screw rpm increases, more work is put into the polymer, and hence, the extent of melt fracture rises (i.e., the surface appearance becomes poorer). This description is illustrated in Fig. 7 which is a plot of machine specific energy versus the viscous temperature rise.

The above means that one can relate surface appearance simply to the machine's specific energy. That is, for a particular polymer a definite relationship exists between skin appearance and energy of extrusion (see Fig. 8). The greater degree of scatter in the correlation compared to Fig. 6 is a reflection of the variance of torque values. At low extrusion temperatures it is more difficult to maintain steady feed to a small extruder. Ideally, the machine's specific energy should be computed from a steady-state or time-averaged torque value for each rpm, but experimental values were simply numerically averaged for each rpm.

Extrusion rate can also be expressed in terms of energy input. Figure 9 shows a plot of mass throughput versus total shear energy for the same polymer. Again, a specific relationship exists for a particular polymer and screw geometry.

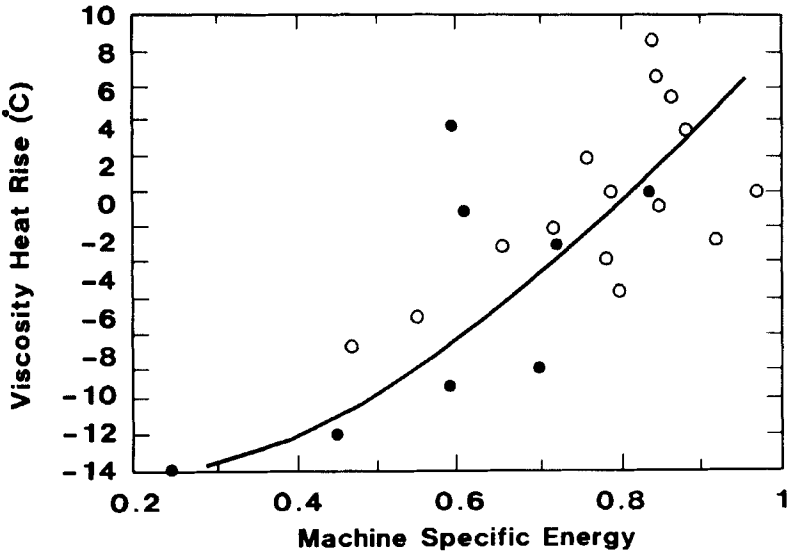

FIG. 7. Energy input vs viscous heating for Polymer A.

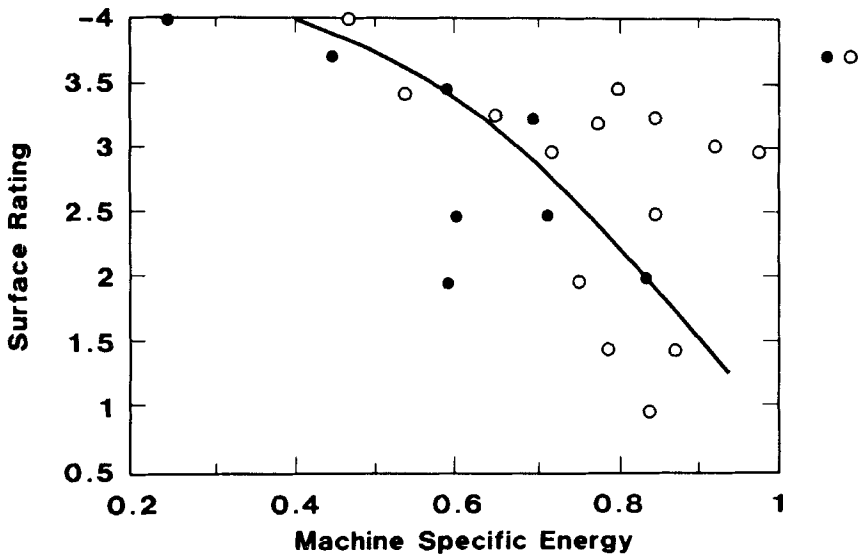

FIG. 8. Energy input level vs surface rating for Polymer A.

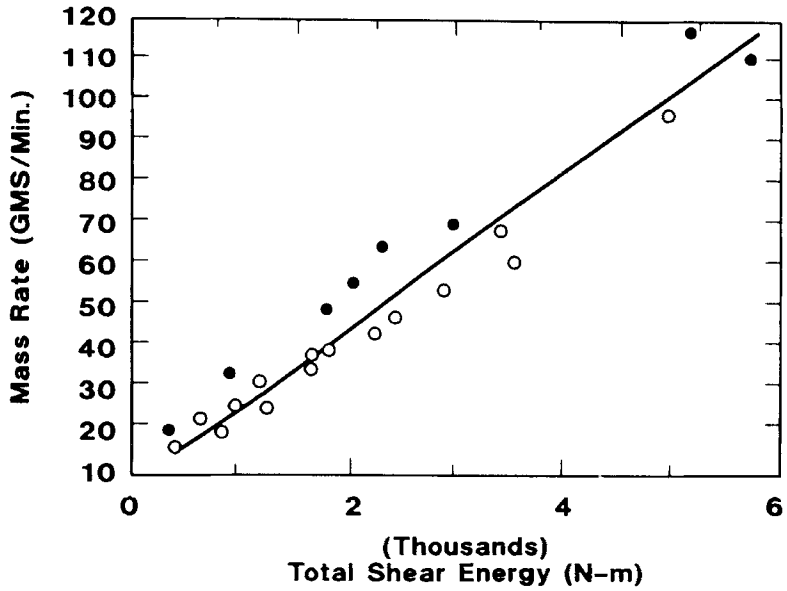

FIG. 9. Mass rate vs machine input for Polymer A.

The importance of screw geometry is illustrated in Figs. 10-12. Figure 10 shows the surface appearance-viscous temperature rise correlation for the same polymer for the three screw geometries described earlier. As shown, the same trends are observed; however, screw geometry can dramatically alter the degree of melt fracture or skin smoothness. Screw geometry essentially establishes the operating curve of the extruder, as shown by the throughput-head pressure curves in Fig. 11. The geometry effect is explained in part by the fact that the polymer melt is subjected to different shear rates along the extruder axis. Figure 12 illustrates this by comparing the theoretical axial shear rates for the three screw geometries used (computed by using Definition 7 and screw geometry tolerances from Fig. 2). This means that the different screws used in this study subject the polymer melt to a different shear rate at the same screw rpm, and therefore the melt viscosity can be different. This is illustrated by the rheological flow curve in Fig. 13, developed for the same polymer over identical screw rpm's by applying constitutive Eqs. (8)-(10). As shown, the processing viscosity varies with shear rate, as expected, and changing screw geometry simply imposes a different shear rate in the melt zone and, hence, affects viscosity.

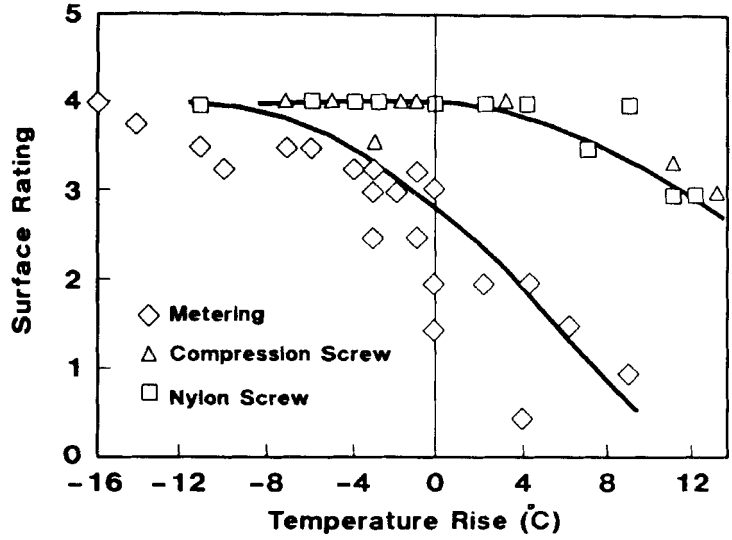

FIG. 10. Screw geometry effect on surface appearance.

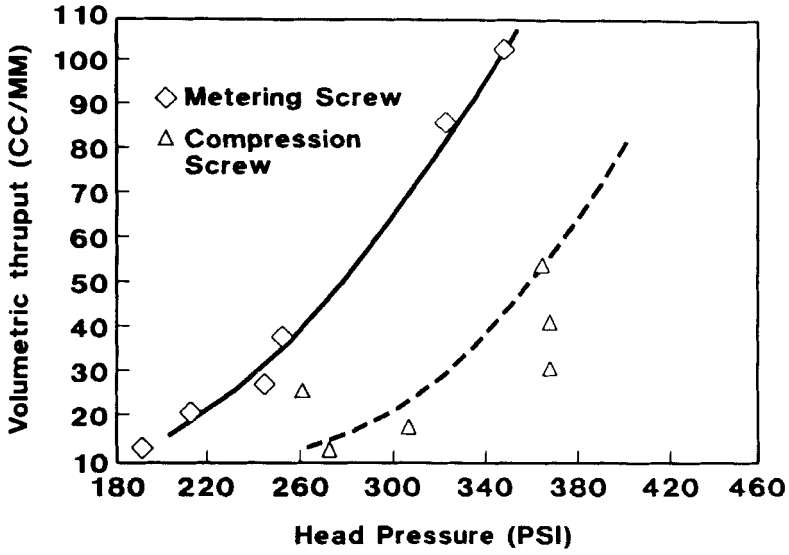

FIG. 11. Operating curves for different screws at 89°C. (145 psi = 1 MPa)

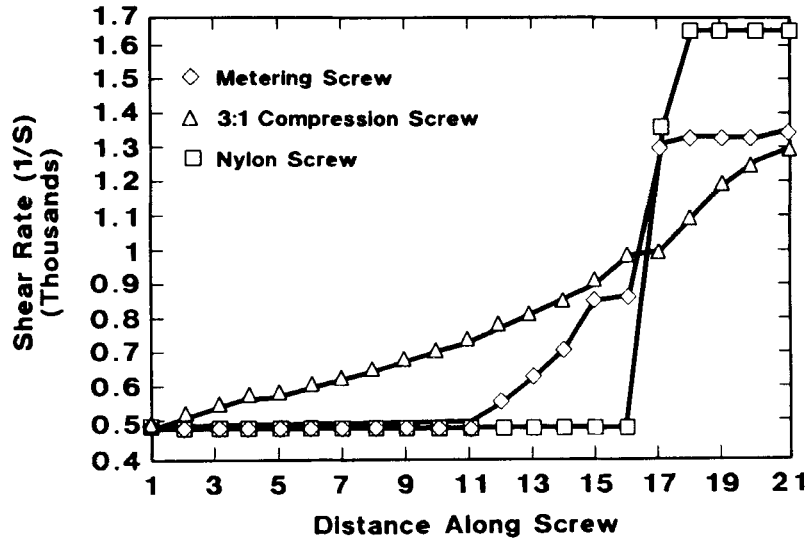

FIG. 12. Theoretical axial shear rate profiles for a 31 rpm screw speed.

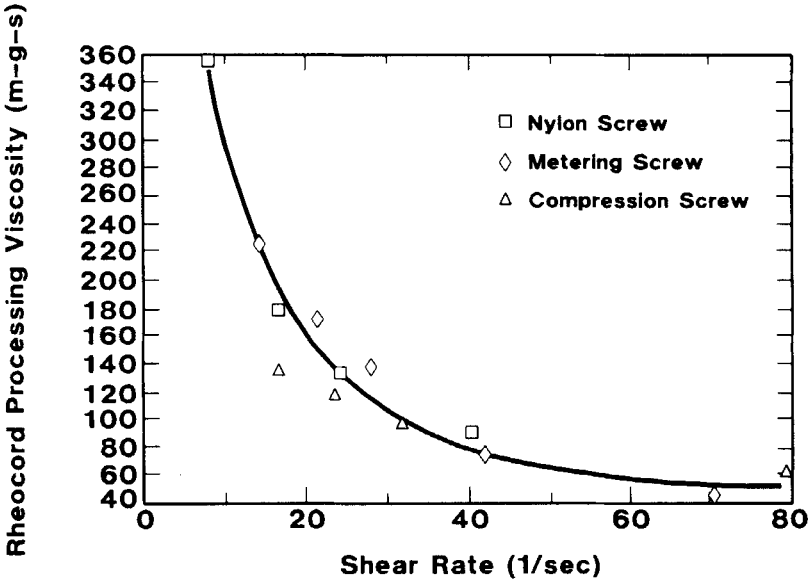

FIG. 13. Viscosity curve generated for different screw configurations.

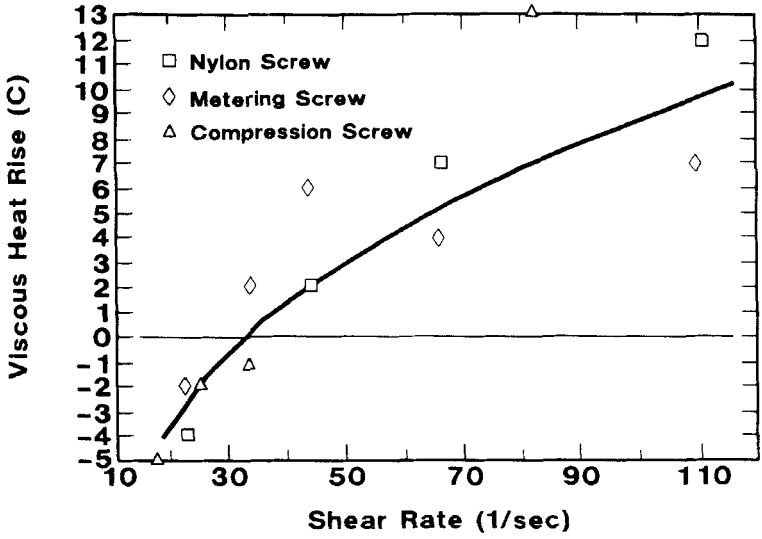

FIG. 14. Viscous heat rise for different screws for Polymer A.

The above observations imply that the degree of melt fracture or skin smoothness is a function of effective shear rate, i.e., the skin appearance data of Fig. 10 should show a unique correlation with shear rate for a particular polymer. Figure 14 illustrates this in terms of the viscous heat rise. This is equivalent to reducing the surface appearance data in Fig. 10 to a single correlation.

Summarizing the principal conclusions up to this point:

1. The rheocord can be applied as a processability tester, relating an empirical processing viscosity to the molecular characteristics of polymers.
2. Scale-up of skin appearance and extrusion performance for different screw geometries seems feasible by properly accounting for effective shear rate.
3. From a hydrodynamic standpoint, skin smoothness appears to be only a function of direct energy input, i.e., the greater the amount of work performed, the greater the viscous heat rise, and consequently, the greater the extent of melt fracture.

COMPARISON OF POLYMER PERFORMANCES

Figure 15 provides a processing map of the various polymers tested. It illustrates some of the relative processing advantages of the polymers tested. For example, EPDM (B), although it shows a surface appearance response similar to A, extrudes at a faster rate for the same screw speed. Hence this polymer would be preferred over Polymer A from a production efficiency standpoint.

Polymers C, E, and F show similar responses, i.e., surface appearance worsens at higher extrusion rates. In contrast, D and J show not only higher extrusion rates and better surface appearance than A, but demonstrate a wider processing latitude in that surface appearance was insensitive to screw speed over the range tested. It should be noted that J is not a viable candidate in a sponge application due to poor physical and cure properties, which, of course, is a key factor in the selection process of a suitable polymer candidate.

The response of Polymer G is of particular interest among the polymers with acceptable sponge performance properties. Although its surface appearance is slightly deficient compared to that of D, its surface appearance re-

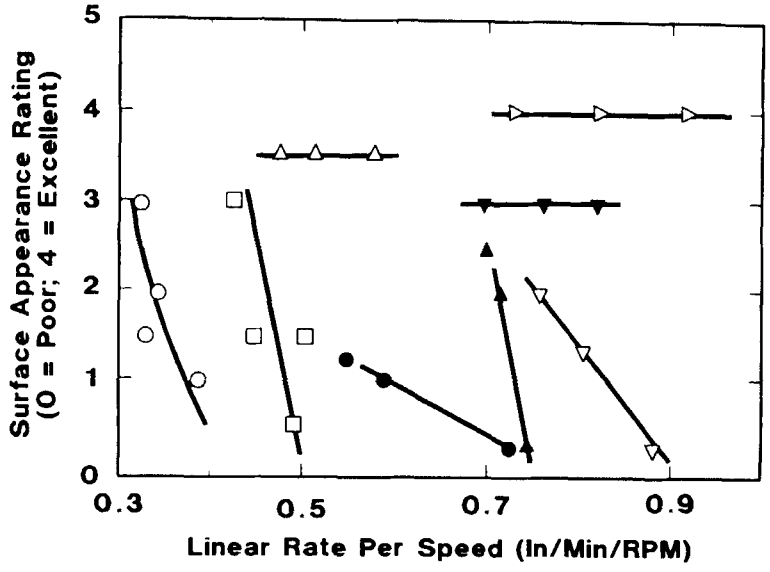

FIG. 15. Processing map. See Table 1 for identification of the symbols.

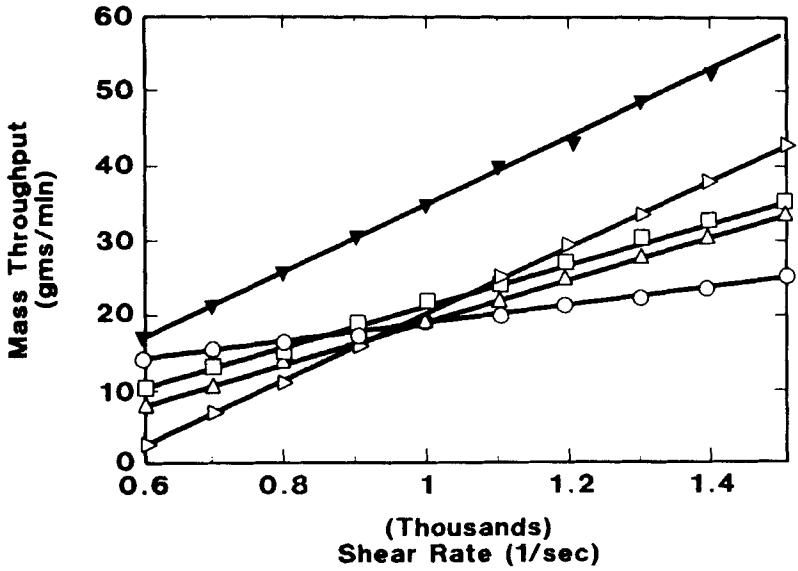

FIG. 16. Mass throughput comparison of polymers. Extrusion temperature: 89°C.

sponse displays the same relative insensitivity to screw speed at higher rates. The wider processing latitude compared to A would suggest a marketing advantabe for this type of EPDM.

A comparison of mass extrusion rates for several of the polymers is shown in Fig. 16. Polymers B, D, and J extrude faster than A in the higher shear rate ranges. In contrast, G is shown to extrude significantly higher than the other polymers at identical shear rates, which is an obvious second processing advantage.

Polymer G, therefore, shows some interesting advantages. Figure 17 provides a comparison of the surface appearances for Polymers G and A over a wide shear-rate range. As shown earlier, G is considerably less sensitive to shear rate (or extruder rpm) than A. A second parameter, extrusion temperature, also helps. As shown, an incremental improvement in surface appearance is achieved with G by increasing extrusion temperature (the higher temperature of extrusion translates into less viscous heating because of a lower melt viscosity). Furthermore, the higher extrusion temperature is feasible for G because there is little to no loss in scorch safety, whereas A is already at the scorch safety limit at the lower extrusion temperature.

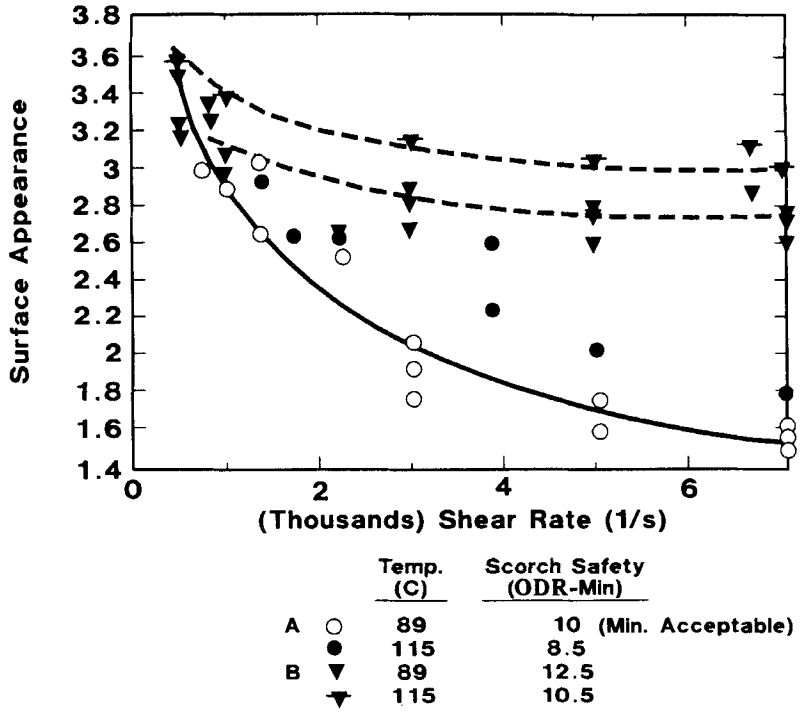

FIG. 17. Surface appearances of two polymers.

Figure 18 provides a cross plot of surface appearance and mass extrusion rate for identical shear rates. G shows a considerably greater processing latitude.

The critical question is how well the data of Fig. 18 correspond to the compounder's observed performance. Depending on operating regime and apparatus configuration, differences may not be as clearly pronounced. Figure 18 does, however, demonstrate that the surface performance of G is not nearly as sensitive to line rates or, more specifically, process conditions of extrusion.

We may conclude that Polymer G should enable the compounder to experiment with extrusion conditions to achieve improved surface performance over A. Specifically, screw speed and wall temperature offer a means of adjusting surface appearance. Since G extrudes faster than A, it may be possible to achieve significant improvement in surface appearance at similar to perhaps improved line rates over A.

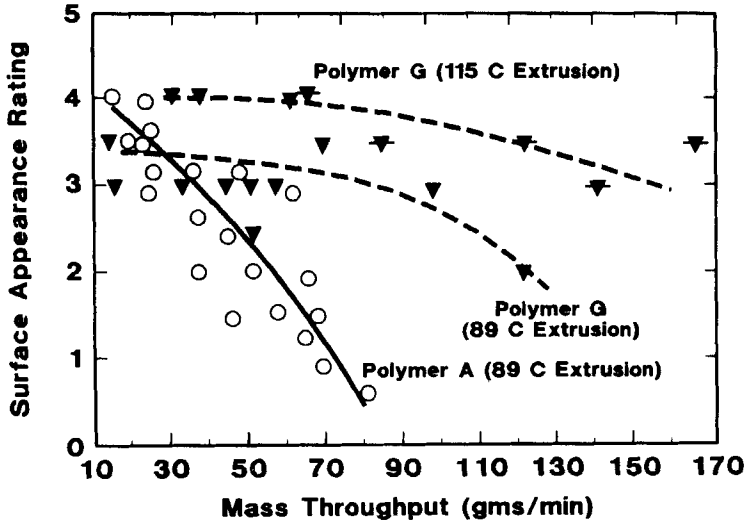

FIG. 18. Comparison of Polymer A to Polymer G performance.

OPTIMIZING PROCESSING PERFORMANCE THROUGH POLYMER DESIGN

An attempt to optimize the performance of G was made by a screening study of molecular variables. In particular, the effects of long-chain branching over a very limited range, overall crystallinity content, and the effect of the high ends of the molecular weight distribution were studied. Table 2 provides a summary of the characteristics of the polymers studied. The last column in this table provides a rating of the degree of branching relative to Polymer G. The lower the value, the more branched the sample is perceived to be.

No difference was observed in extrusion rate between variants of Polymer G. Figure 19 shows that all candidates extruded significantly faster than A. This means that all the samples are the same rheologically, and this is illustrated in the viscosity curves of Fig. 20. This behavior can be attributed to the high levels of branching in all the candidates. In general, most of the candidates showed similar levels of branching (all relatively high). Furthermore, the ethylene contents of all polymer variants were higher than that of Polymer A, suggesting better cold green strength, which explains the faster extrusion

TABLE 2. Summary of Polymer Properties Prepared as Variants of Polymer G

Polymer identification	Symbol on plots	$\bar{M}_w$	$\bar{M}_z$	Polydispersity $\bar{M}_w/\bar{M}_n$	Branching index relative to G
F	▲	266 000	1 448 000	4.67	0.84
G	▼	278 000	1 735 000	4.28	1.00
K	○	287 000	1 628 000	5.25	0.65
L	○	389 000	4 278 000	6.05	0.30
M	○	302 000	2 356 000	4.65	0.86
N	■	380 000	4 989 000	6.13	0.39
O	◇	378 000	5 374 000	5.90	0.30
P	◆	369 000	6 140 000	6.78	1.00

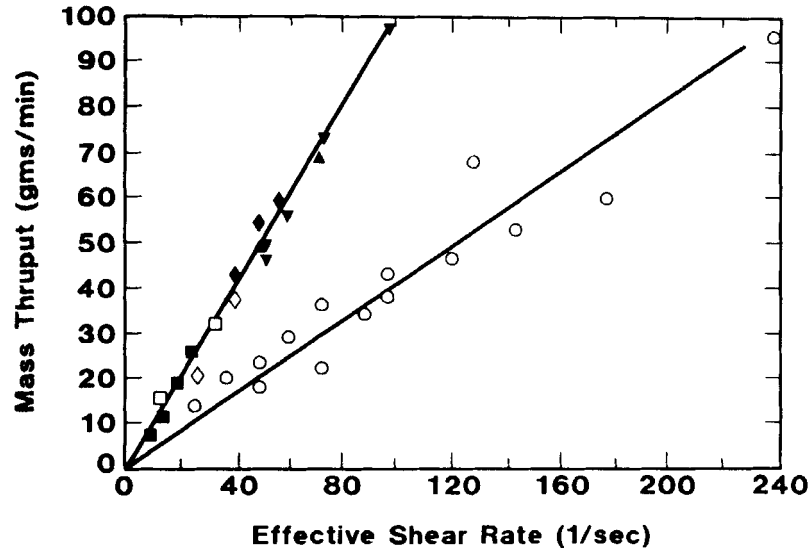

FIG. 19. Extrusion rates for Polymer G variants vs Polymer A.

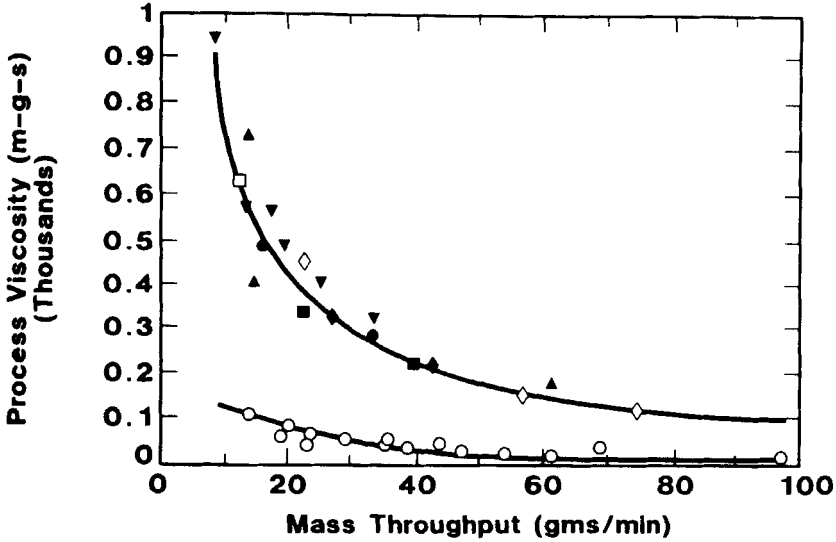

FIG. 20. Comparison of rheological flow curves at 89°C.

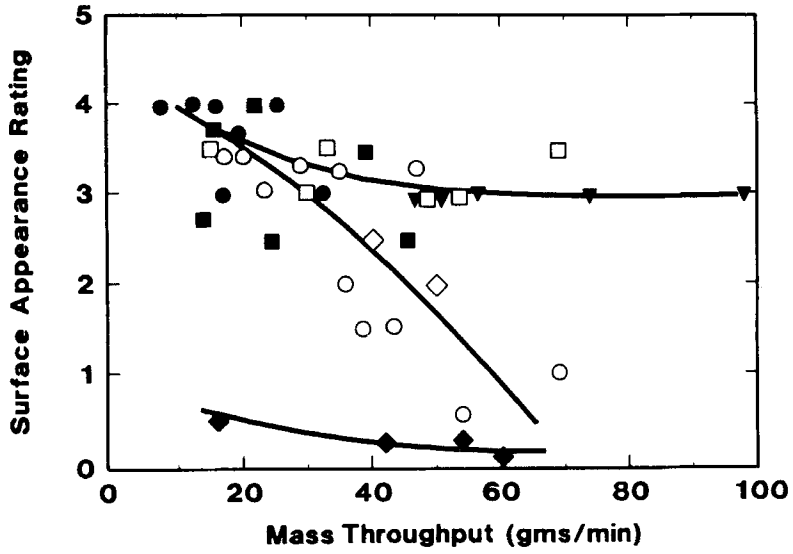

FIG. 21. Comparison of surfaces of Polymer G variants with Polymer A.

rates. Higher green strength translates into more uniform feeding at the inlet of the extruder.

Figure 21 provides a plot of surface appearance rating versus mass throughput. The figure reveals several trends:

1. The slightly less branched polymers show a sensitivity more closely approximating the behavior of Polymer A. That is, there is a loss in surface appearance at higher shear rates (or throughputs).
2. Despite a wide range of higher $\bar{M}_z$ (high mode of the molecular weight distribution) based on gel permeation chromatography, the same overall surface response is observed. We conclude that the surface performance is not sensitive to the size of the molecular weight distribution tail over the range tested.
3. The broadest polymer is clearly the worst candidate and supports the belief that the desired product must not exceed some maximum breadth of distribution.

The final observation, to be consistent with earlier discussions, is given in Fig. 22, which is a plot of mass throughput versus viscous heat rise, showing that

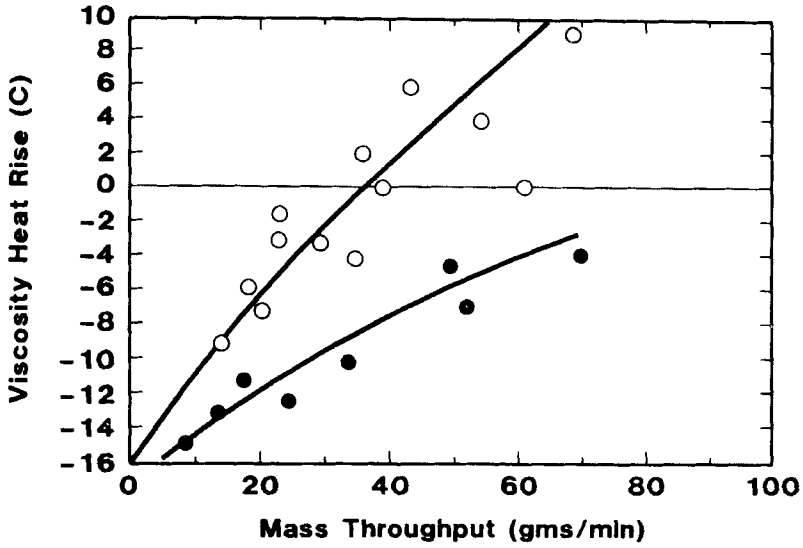

FIG. 22. Viscous heat rises.

the G candidate in general experiences less heat build-up than A, and consequently melt fracture should be lower, which accounts for the improved surface appearance.

RHEOLOGICAL AND MOLECULAR PARAMETERS AFFECTING EXTRUSION PERFORMANCE

The advantages of a "tailored" molecular weight distribution to overall extrusion performance was described earlier [1]. As shown, extrusion performance can be related to molecular weight distribution, in particular and polydispersity ratios of $\bar{M}_w/\bar{M}_n$ and $\bar{M}_z/\bar{M}_w$ and overall molecular weight. Rheological behavior can be related to these parameters to provide guidance in achieving the desired melt viscosity in the melt and pumping sections of the extruder, which, in turn, can be related to mass throughput performance.

Insufficient data were generated to develop a quantitative understanding of the molecular parameters affecting surface appearance, but one important trend was observed. Figure 23 provides plots of the overall surface performance versus the number average molecular weight and the z-to weight-average

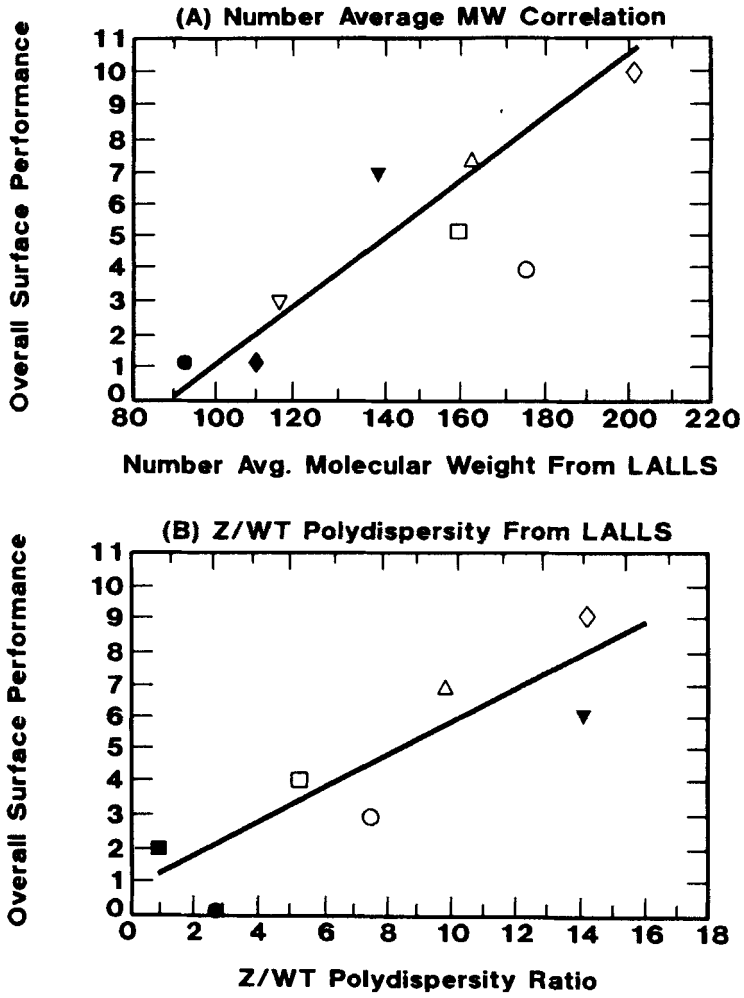

FIG. 23. Effect of breadth of MWD on surface appearance.

polydispersity. The performance ordinate is a qualitative assessment of the overall surface appearance or rating over the entire range of experimental conditions (i.e., a qualitative rating between samples was made on a scale of 1 to 10, where 10 is the best). As shown, overall surface appearance improves with higher molecular weight, and notably with higher ends of the distribution.

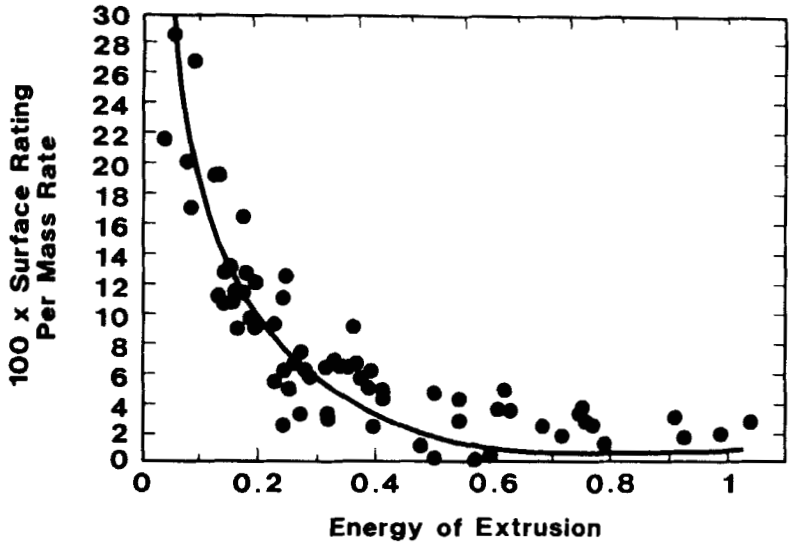

FIG. 24. Generalized correlation for surface appearance.

This could mean that the high MW ends impart longer relaxation times and, hence, a lower degree of fracture is observed at the die exit.

In this study we have attempted to gain an understanding of how both end-use processing conditions and molecular structure interact on overall extrusion performance. The study has shown that effective shear rate and extrusion wall temperature can dramatically alter skin appearance below the physical limitations of scorch. This observation can be summarized by the universal processing plot developed in Fig. 24. This plot was constructed from data obtained for all the polymers tested, over extrusion temperatures ranging from 89 and 135°C and for three different screw geometries. Basically, the correlation illustrates that surface response and extrusion performance are simply functions of the overall energy input to the apparatus. That is, the desired skin appearance can be achieved for any polymer depending on energy input. The question remains whether that particular polymer meets end-use property requirements over the specified process range of the extruder.

SUMMARY

The principal observations of this study are as follows: Broad molecular weight distribution (MWD) polymers appear to offer a wider processing lati-

tude in terms of surface appearance at higher throughput rates. Surface response appears less sensitive to throughput than for narrow MWD polymers. This, coupled with a higher level of scorch safety, suggests incremental improvement in skin appearance can be achieved by extruding at higher temperatures. In contrast, linear, narrower MWD polymers result in poorer surface appearance.

The rheocord has been demonstrated to be a reliable processability tester, and constitutive equations relating to processing performance have been developed. Integration of this instrument into product optimization is essential for the product designer.

NOTATION

D	screw diameter
E	activation energy
F	force
h	gap between screw and barrel
K	unit shear viscosity
k	Arrhenius coefficient
MWD	molecular weight distribution
$\bar{M}_w$	weight-average molecular weight
$\bar{M}_n$	number-average molecular weight
$\bar{M}_z$	z-average molecular weight
m	mass throughput
N	screw speed
n	power law exponent
P	power
r	radius
R	universal gas law constant
SE	specific energy
SO	specific output
T	absolute temperature
TE	total shear energy
V	rotational velocity
$\dot{\gamma}$	shear rate
τ	shear stress

REFERENCES

[1] N. P. Cheremisinoff, *Polymer Mixing and Extrusion Technology,* Dekker, New York, 1987.

[2] N. P. Cheremisinoff, "Predicting the Extrusion Performance of EPDMs," *Polym.-Plast. Technol. Eng., 27*(1) (1988).

[3] N. P. Cheremisinoff and C. B. Shulman, *Study of the Hydronamic and Viscoelastic Properties Affecting the Surface Appearance of Extruded EPDM Compounds,* SAE Conference Paper, Detroit, March 1989.

[4] J. T. Chung, "Introduction to Torque Rheometry," *Encyclopedia of Fluid Mechanics,* Vol. 7 (N. P. Cheremisinoff, ed.), Gulf Publishing Co., Houston, 1988.

[5] R. Keller and N. P. Cheremisinoff, *New Developments in Ethylene-Propylene Elastomers for Extruded Applications,* Paper Presented at Rubberex 86, Australasian Rubber Conference, Melbourne, Australia, April 29, 1986.

[6] C. B. Shulman, *Unique Features of High Unsaturation EPDM Polymers,* Paper Presented at 128th Rubber Division Meetings, Cleveland, Ohio, October 1985.

[7] G. Stella and N. P. Cheremisinoff, *Designing EPDM's for Production Efficiency,* Paper Presented at International Rubber Conference–Rubbercon 88.

Received December 29, 1988